

# Ultrafast Energy Transfer between Disordered and Highly Planarized Chains of Poly[2-methoxy-5-(2-ethylhexyloxy)-1,4-phenylenevinylene] (MEH-PPV)

Thomas Unger,<sup>†,‡</sup> Fabian Panzer,<sup>†,‡</sup> Cristina Consani,<sup>§</sup> Federico Koch,<sup>§</sup> Tobias Brixner,<sup>§,||</sup> Heinz Bässler,<sup>‡</sup> and Anna Köhler<sup>\*,†,‡</sup>

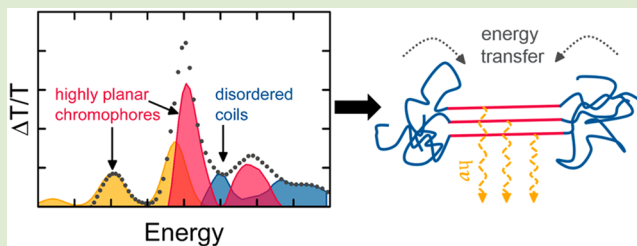
<sup>†</sup>Experimental Physics II, University of Bayreuth, 95540 Bayreuth, Germany

<sup>‡</sup>Bayreuth Institute of Macromolecular Research (BIMF), University of Bayreuth, 95440 Bayreuth, Germany

<sup>§</sup>Institut für Physikalische und Theoretische Chemie and <sup>||</sup>Center for Nanosystems Chemistry (CNC), Universität Würzburg, Am Hubland, 97074 Würzburg, Germany

## Supporting Information

**ABSTRACT:** Upon cooling a solution of poly[2-methoxy-5-(2-ethylhexyloxy)-1,4-phenylenevinylene] (MEH-PPV), a phase transition occurs, leading to the formation of aggregates. We have studied the dynamics of singlet excitons in MEH-PPV solution below the critical temperature of the phase transition using steady-state photoluminescence measurements and pump–probe fs-spectroscopy at different temperatures. Spectral analysis indicates the coexistence of disordered chromophores with highly planarized chromophores. The high planarity is evidenced by a remarkably high 0–0/0–1 peak ratio in the spectra. By spectrally separating the contributions of either type of chromophore to the pump–probe signal we find that energy transfer takes place within less than 1 ps from disordered, unaggregated chain segments to highly planarized, aggregated chain segments. The short time scale of the energy transfer indicates intimate intermixing of the planarized and disordered polymeric chromophores.



Conjugated polymers are prone to aggregation in solution.<sup>1–3</sup> Below a critical transition temperature that depends on the chain length,<sup>4</sup> isolated and more or less coiled chains tend to aggregate with a concomitant increase of their effective conjugation length. A manifestation of this phenomenon is the appearance of lower-energy absorption and fluorescence bands so that the spectra exhibit an isosbestic point. Absorption spectra demonstrate, nevertheless, that both phases coexist well below the phase transition temperature with the fractional contribution of the ordered phase increasing upon further cooling. On the other hand, the fluorescence comes almost exclusively from the ordered phase. This is a signature of efficient energy transfer between both phases.

The purpose of the current work was to unravel the interplay between the disordered and ordered phases, identify the nature of both phases and measure of rate of energy transfer between them. As a test material, we chose MEH-PPV in solution as a prototypical  $\pi$ -conjugated polymer for which a wealth of information is already existing, employing steady-state absorption and fluorescence spectroscopy, as well as time-resolved pump–probe spectroscopy within a broad temperature range. Based on spectral decomposition techniques and adopting Spano et al.'s H/J-aggregate model,<sup>5</sup> we are able to associate the room temperature phase with disordered chains or chain segments, while, in the aggregated phase, chains or chain segments prevail that are extended with predominant J-type

character. From the observation that energy transfer from the disordered to the planarized chromophores occurs on a subps time scale we will conclude that both types of chromophores are intimately connected, for example, by forming an array of extended chains surrounded with a “hairy” surface of coiled chains.

For the investigation, we used MEH-PPV that was purchased from American Dye Source Ltd. (ADS). It was dissolved in methyltetrahydrofuran (MTHF) at a concentration of 0.2 mg/mL. To ensure that all of the polymer chains are completely dissolved, the solution was heated to 50–60 °C and stirred for about 10 h until no macroscopic particles could be observed. The experiments were performed in a temperature range between 300 and 120 K where MTHF is liquid.<sup>6</sup> Steady-state absorption and emission spectra at different temperatures were recorded with a home-built setup. The solutions were filled into a 1 mm fused silica cuvette and put in a temperature-controlled continuous flow cryostat (Oxford Instruments). In order to minimize the light intensity impinging on the sample, we used two correlated monochromators for incident as well as transmitted light. The latter was recorded by a silicon diode and a lock-in-amplifier.

Received: February 19, 2015

Accepted: March 26, 2015

Published: March 30, 2015

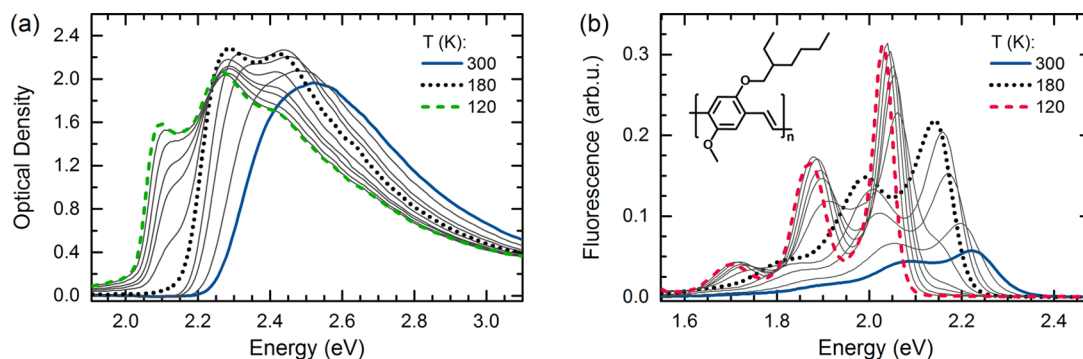


**Figure 1.** Steady-state (a) absorption and (b) fluorescence spectra of MEH-PPV in MTHF for different temperatures, that is, at 300, 260, 220, 200, 180, 175, 170, 165, 155, 140, and 120 K. Fluorescence spectra were corrected for the relative changes in absorption at the excitation energy (3.06 eV).

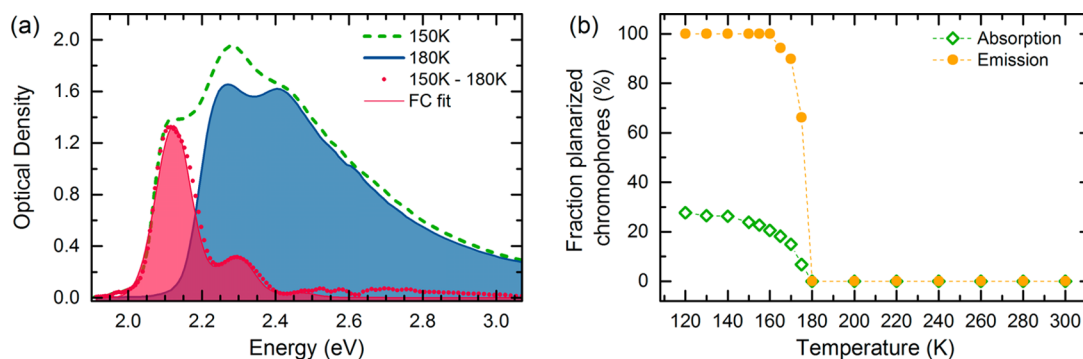


**Figure 2.** (a) Absorption spectrum at 150 K (green dashed line) together with the absorption spectrum of the disordered phase (filled blue curve) that was measured at 180 K and subsequently normalized to match the high energy tail of the 150 K absorption spectrum. The difference between the 150 and 180 K spectra is shown by the red dots. This difference spectrum can be reproduced by a Franck–Condon progression (filled red curve). (b) Fraction of planarized chromophores as a function of temperature obtained from the absorption spectra (open green diamonds) and from the emission spectra (orange dots), as described in the Supporting Information.

For steady-state emission measurements, the xenon lamp and the first monochromator were replaced via a shutter by a diode laser with an excitation wavelength at 405 nm (3.06 eV), exciting the sample at a shallow angle. Emission was recorded by the same detection unit. This ensured recording absorption and fluorescence spectra at the same sample spot and temperature immediately after one another. All spectra were corrected for the transmission of the setup, using an Oriel calibration lamp. Sample heating or cooling was done in a stepwise fashion with a heating or cooling rate of 2 K per min and waiting 30 min before taking the measurement at a given temperature to ensure thermal equilibrium within the sample.

The transient absorption data with excitation at 2.48 eV (pulse length 190 fs) were obtained using a 100 kHz setup from Coherent Ltd., as described in more detail in the Supporting Information (SI). In brief, the pump-pulse fluence was set to about  $10 \mu\text{J}/\text{cm}^2$  to keep the pump-probe signal linear with fluence (see Figure S1). The spectra were recorded using a lock-in amplifier and a monochromator with a silicon diode. To obtain transient absorption data with excitation at 2.12 eV (pulse length 42 fs), a 1 kHz setup from Spectra Physics was employed. Here also excitation pulse energies were low enough to keep the signal in the linear regime.

Figure 1 shows the absorption and photoluminescence (PL) spectra of MEH-PPV in MTHF solution in the temperature range between 300 and 120 K. In absorption, the 300 K spectrum is vibrationally unresolved with a maximum at 2.5 eV (Figure 1a). It is associated with disordered coil-like polymer

chains.<sup>7–9</sup> Upon cooling to 180 K, the spectra shift to the red by about 80 meV. They continuously acquire vibrational structure and a 0–0 feature near 2.3 eV develops. In contrast, the emission spectrum at 300 K shows vibrational structure with  $S_1 \rightarrow S_0$  0–0, 0–1, 0–2 peaks at 2.23, 2.07, and 1.89 eV, respectively (Figure 1b). When lowering the temperature from 300 to 180 K, the spectra shift to the red by about 80 meV similar to the behavior in absorption. This is accompanied by a continuous increase in overall intensity, where the area beneath the spectrum at 180 K more than triples compared to the area at 300 K (see Figure S2 in SI for energetic shifts of the  $S_1-S_0$  0–0 peak and area under the spectra as a function of temperature). Thus, upon cooling until 180 K, absorption and emission spectra shift to the red and become more intense. This indicates that the conjugated segments of the chain become more extended, although their overall chain conformation still corresponds to that of a disordered coil conformation.<sup>4,10,11</sup> This is similar to the behavior that was recently observed when cooling solutions of P3HT,<sup>2,4</sup> as well as PCPDTBT.<sup>12</sup>

When further cooling below 180 K, a new absorption (emission) peak near 2.1 eV (2.05 eV) appears and grows in intensity at the expense of absorption (emission) from coiled chains. It is assigned to the absorption (emission) of planarized MEH-PPV chain segments in aggregates.<sup>7</sup> Below 170 K, emission from the coiled chains vanishes and the fluorescence spectrum is dominated by the planarized chromophores. This is consistent with earlier work,<sup>7</sup> and has been attributed to the

occurrence of a disorder–order transition. The PL spectra of the planarized chromophores bear out a bathochromic shift from 2.053 to 2.026 eV upon further cooling from 170 to 120 K and the associated absorption spectra shift by the same amount (Figure S2).

To gain detailed information about the absorption from the planarized chains or chain segments requires decomposition of the measured spectra below 180 K. Here we followed a scaling approach, similar to that in Reference 13, which we already used for decomposing absorption spectra of aggregated P3HT in solution.<sup>2,4</sup> This approach is applicable to MEH-PPV because the spectra bear out an isosbestic point at 2.24 eV in the temperature range of 180 to 140 K (Figure 1a), which is an unambiguous evidence that a transition from a coiled to an ordered phase is occurring.<sup>14,15</sup> Figure 2a illustrates the decomposition approach and shows the measured absorption spectrum at 150 K (green dashed line) together with the normalized absorption spectrum of the disordered phase measured at 180 K (filled blue curve). The difference between these spectra (red dots) is attributed to absorption from planarized chromophores with peaks at 2.1 and 2.3 eV. A Franck–Condon analysis of this absorption spectrum (filled red curve) from the planarized chromophores yields a Huang–Rhys parameter of  $S = 0.25$ , an  $I_{0-0}/I_{0-1}$  ratio = 4, an effective vibrational mode of  $E_d = 170$  meV and a Gaussian line width of  $\sigma = 48$  meV. In the framework of the H/J-aggregate model developed by Spano and co-workers,<sup>5</sup> such a high  $I_{0-0}/I_{0-1}$  ratio is a signature of strong coupling along the polymer chain (intrachain) in the aggregated phase and correspondingly weak coupling between different polymer chains (interchain). The same high ratio applies to coupling along a linear arrangement of chromophores and to coupling between chromophores in an adjacent, face-to-face arrangement, respectively. Similar remarkably high  $I_{0-0}/I_{0-1}$  ratios have been observed for fully planarized single crystals of P3HT.<sup>16</sup> This appears to be a signature of ordered domains of  $\pi$ -conjugated chains in general, tractable in terms of Spano et al.'s theory.<sup>5</sup> The fraction of planarized chromophores as a function of temperature is displayed in Figure 2b. It was obtained from the absorption fraction of planarized chain segments, taking into account the relative change in oscillator strength between disordered and planarized chain segments, as detailed in the SI.

From the absorption data we infer that below the critical transition temperature, the percentage of planarized chromophores increases continuously, saturating at a maximum value of about 30% at 120 K. In contrast, the percentage of fluorescence from planarized chromophores increases steeply below the transition temperature, until below 160 K, emission results entirely from the planarized chromophores. The fact that emission results entirely from planarized chromophores though they make up only 30% of the total composition implies efficient energy transfer from disordered to planarized chromophores.

Figure 3 shows the transient absorption spectrum of MEH-PPV in solution at 120 K, excited at 2.12 eV and probed between 2.5 and 1.7 eV with a delay time of 75 fs. As the disordered chains do not absorb for excitation at 2.12 eV, we assign the peak observed near 2.3 eV to the ground-state bleach (GSB) of the  $S_1 \rightarrow S_0$  0–1 transition of the planarized chromophores. The feature near 2.1 eV is the superposition of the ground-state bleach of the 0–0 transition of the planarized chromophores (as evident from Figure 1a) and the associated stimulated emission (SE). Accordingly, the feature centered

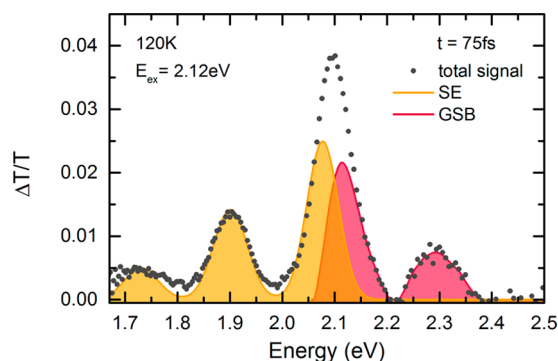


**Figure 3.** Pump–probe spectrum (gray dots) taken at 120 K, 75 fs after excitation at 2.12 eV, where only the planarized chains absorb. The spectrum is decomposed into the contributions from stimulated emission (SE, filled orange curve) and ground-state bleach (GSB, filled red curve). The SE contribution was obtained by normalizing the 120 K PL spectrum to match the 1.9 eV SE peak. The GSB contribution was obtained by subtracting the normalized 120 K PL spectrum from the total  $\Delta T/T$  signal.

near 1.9 eV is assigned to the 0–1 feature of the stimulated emission transition (SE 0–1). Since the fluorescence spectrum of the planarized chromophores is evident in Figure 1b, it is possible to spectrally decompose the 0–0 feature of the pump–probe spectrum into the contributions from GSB and SE. To this end, we take the 120 K photoluminescence (PL) spectrum and normalize it in such a way that the 0–1 peak of the PL spectrum matches the 1.9 eV  $\Delta T/T$  signal in intensity, taking into account a slight spectral shift of about 10 meV between the steady-state and the time-resolved spectra. Subtraction of the 120 K PL spectrum from the  $\Delta T/T$  signal yields the spectrum associated with the ground-state bleach.

From this spectral decomposition we find a 0–0/0–1 ratio of the GSB that significantly exceeds unity, similar to that of the absorption spectra obtained for the planarized chromophores from steady-state data (Figure 2a). In a recent publication,<sup>17</sup> absorption spectra of aggregated MEH-PPV were simulated theoretically resulting in a significantly smaller 0–0/0–1 ratio compared to this work, mainly due to an underestimated contribution of the coiled phase to the overall absorption spectrum.

When exciting a sample held at 120 K with 2.48 eV, Figure 2a tells us that 95% of the absorbing chromophores are in a disordered conformation. Yet already at 1 ps after excitation, the GSB signal shows signatures of both disordered and planarized chromophores. This is documented by Figure 4 in which pump–probe spectra are shown that are detected after a delay time of 1 and 5 ps.

Spectra at further delay times are listed in the SI. Based on the same decomposition routine as above, the total GSB signal, due to disordered chromophores and to planarized chromophores, was obtained. We then used the GSB signal from the planarized chains derived in Figure 3, normalized it appropriately, and subtracted it from the total GSB signal to derive the GSB contribution of the disordered chain, analogous to the spectral decomposition approach described above. The relative contribution of planarized and of disordered chromophores obtained by this procedure is displayed in Figure 5 as a function of time. In both, Figures 4 and 5, we see that the contribution due to the lower-energy, planarized chromophores grows at the expense of the higher-energy, disordered chromophores.

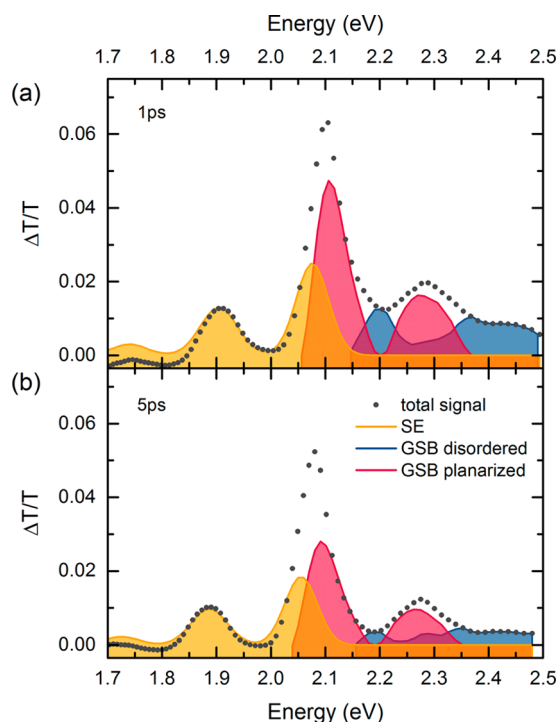


**Figure 4.** Pump–probe spectra for excitation at 2.48 eV (where coiled chains absorb) at 120 K for different time delays after excitation, that is, (a) 1 and (b) 5 ps. In addition to the total  $\Delta T/T$  signal (dots), the contributions of SE, GSB from disordered chromophores, and the GSB from the planarized chromophores are indicated by orange, blue, and red solid lines, respectively.

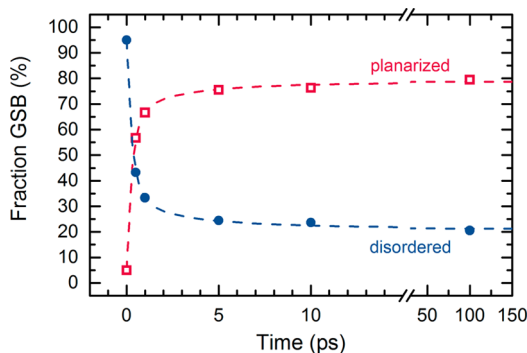


**Figure 5.** Percentage of the ground-state bleach signal that is due to planarized chromophores (open square symbols) or to disordered chromophores (filled round symbols) as a function of time. The dashed line is a guide to the eye, indicating a decay/growth pattern with an initial exponential decay/growth, followed by a stretched-exponential decay/growth.

We interpret the rising contribution from the planarized chromophores to result from energy transfer from the higher-energy disordered chromophores that is completed within a few ps. A similarly rapid energy transfer from disordered to ordered chain segments has been observed also in polyfluorene (PFO) thin films.<sup>18</sup> Such a fast transfer is incompatible with long-range energy transfer from isolated coiled chains to planarized chains (see SI). It rather suggests that planarized and coiled chromophores are in close proximity, for example, by planarized chain segments forming an ordered cluster surrounded by more disordered coiled chains or chain segments, which was also proposed recently.<sup>19,20</sup> Since

experimental and theoretical previous work suggests that MEH-PPV forms planarized segments above a certain concentration,<sup>7,21</sup> the planarized segments are more likely to arise from coalescing chains than by self-folding.

In structures where acceptor chromophores are embedded in a matrix of donor chromophores, energy transfer is characterized by a kinetics comprising several components.<sup>22–24</sup> Initially, fast monoexponential decay of the donor emission prevails due to energy transfer to immediately adjacent acceptor sites. In a second step, the decay becomes dispersive since energy transfer takes place over a range of distances and in a multistep fashion. Both transfer types, that is, (parallel) transfer over a range of distances and (sequential) multistep transfer, have been shown to result in a stretched-exponential decay law,<sup>25–31</sup> also referred to as Kohlrausch–Williams–Watts (KWW) decay law<sup>32</sup>

$$I(t) = I_0 \exp \left[ - \left( \frac{t}{t_0} \right)^\beta \right]$$

where  $\beta$  is a parameter that accounts for the deviation from nonexponentiality.  $\beta$  takes the value of 0.5 in the case of Förster-type energy transfer. In the long-time limit, finally, the donor decay is dominated by those donor chromophores that decay naturally before energy transfer to distant acceptor sites can occur. The donor emission thus asymptotically approaches the natural donor decay lifetime. Figure 5 indicates that the temporal evolution of the GSB contributions of disordered chromophores and of planarized chromophores is consistent with such a picture. The dashed lines indicate such a decay/growth pattern with an initial exponential decay/growth with about 300 fs lifetime, followed by a stretched-exponential with  $\beta = 0.5$  and a characteristic time in the range of 1 ps. Similar values and quality of fit result when using a multiexponential approach.

In passing we mention that, in Figure 4, we consider that the slight difference between the measured  $\Delta T/T$  signal at 1.75 eV and the SE (derived from the normalized PL spectra) indicates some excited-state absorption from disordered chromophores.

We now consider the decay of the pump–probe signal near 2.1 eV. This is interpreted as the decay of the excitations on the planarized segments. Figure 6 reveals a decay that is not exactly exponential yet approaches an exponential decay with a lifetime of about 350 ps. Such deviation from monoexponentiality is an ubiquitous phenomenon not only in energy-transfer studies but also in time-resolved fluorescence studies on conjugated polymers.<sup>24</sup> It is usually associated with residual trapping at unidentified traps such as oxidation products with a time-dependent trapping rate that translates into a dispersive decay law, described in terms of the Kohlrausch–Williams–Watts (KWW) decay law,<sup>32</sup> mentioned above. An exponent of 0.8 indicates that a small fraction of aggregate excitations are lost via a weakly dispersive exciton motion toward unidentified scavengers such as electron traps that are ubiquitous in  $\pi$ -conjugated polymers.<sup>33–35</sup>

In conclusion, in addition to the observed ultrafast energy transfer and implied core–shell structure of the aggregates, an intriguing aspect of the present work relates to the decomposition of the absorption spectra of MEH-PPV in MTHF solution near and below the transition temperature. At first glance, the overall spectra shown in Figure 2 resemble the absorption spectra of weakly interacting H-aggregates in P3HT, bearing out an apparent ratio of the 0–0 and 0–1 features of

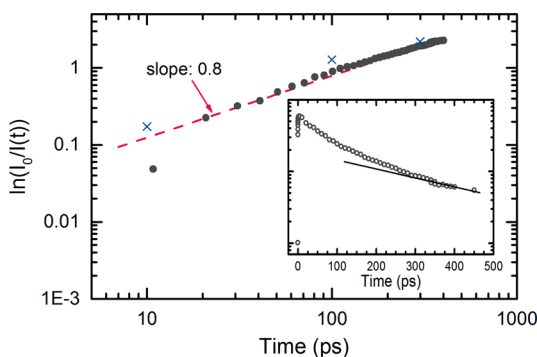


**Figure 6.** Decay of  $\Delta T/T$  at 2.07 eV (dots) for  $E_{\text{ex}} = 2.48$  eV at 120 K, presented in a Kohlrausch–Williams–Watts (KWW) plot for times  $>10$  ps. The red dashed line indicates a slope of 0.8, as discussed in the text. For comparison, the blue crosses indicate the values obtained for the area below the GSB + SE 0–0 band centered at 2.1 eV (=zeroth spectral moment). Slight deviation at early time scales originate from a spectral band shift. The inset shows  $\Delta T/T$  at 2.07 eV plotted in a semilogarithmic fashion, with the solid line indicating a mono-exponential decay function with a lifetime of 350 ps.

less than unity. Separating those spectra disproves this conjecture. It turns out that the isolated spectrum of the planarized chromophores is mirror-symmetric with the fluorescence spectrum, thus, implying a high planarity of the aggregated chains. In fact, comparison of the emission spectra indicates the planarized chromophores in MEH-PPV to be as planar as ladder-type poly(*p*-phenylene) (MeLPPP), where covalent bridges enforce a rigid, flat structure and which recently has shown room temperature Bose–Einstein condensation of cavity exciton-polaritons.<sup>36</sup>

## ■ ASSOCIATED CONTENT

### ● Supporting Information

Details on transient absorption setup. Relative change of area under emission spectra and spectral shift of emission and absorption as a function of temperature. Details on the calculation of the fraction of planarized chains, relative change of oscillator strength as a function of temperature. Transient absorption spectra for further times after excitation. Estimation of energy transfer range. This material is available free of charge via the Internet at <http://pubs.acs.org>.

## ■ AUTHOR INFORMATION

### Corresponding Author

\*E-mail: [anna.koehler@uni-bayreuth.de](mailto:anna.koehler@uni-bayreuth.de).

### Notes

The authors declare no competing financial interest.

## ■ ACKNOWLEDGMENTS

We acknowledge financial support by the Bavarian State Ministry of Science, Research, and the Arts through the Collaborative Research Network “Solar Technologies go Hybrid”, by the German Science Foundation DFG through the doctoral training center GRK1640 and by the Federal Ministry of Education and Research (BMBF) through the Project “OLYMP”.

## ■ REFERENCES

(1) Yamagata, H.; Hestand, N. J.; Spano, F. C.; Köhler, A.; Scharsich, C.; Hoffmann, S. T.; Bäessler, H. *J. Chem. Phys.* **2013**, *139*, 114903.

(2) Scharsich, C.; Lohwasser, R. H.; Sommer, M.; Asawapirom, U.; Scherf, U.; Thelakkat, M.; Neher, D.; Köhler, A. *J. Polym. Sci., Part B: Polym. Phys.* **2012**, *50*, 442–453.

(3) Cone, C. W.; Cheng, R. R.; Makarov, D. E.; Vanden Bout, D. A. *J. Phys. Chem. B* **2011**, *115*, 12380–12385.

(4) Panzer, F.; Bäessler, H.; Lohwasser, R.; Thelakkat, M.; Köhler, A. *J. Phys. Chem. Lett.* **2014**, *5*, 2742–2747.

(5) Yamagata, H.; Spano, F. C. *J. Chem. Phys.* **2012**, *136*, 184901.

(6) Aycock, D. F. *Org. Process Res. Dev.* **2007**, *11*, 156–159.

(7) Köhler, A.; Hoffmann, S. T.; Bäessler, H. *J. Am. Chem. Soc.* **2012**, *134*, 11594–11601.

(8) Mirzov, O.; Scheblykin, I. G. *Phys. Chem. Chem. Phys.* **2006**, *8*, 5569–5576.

(9) Schwartz, B. J. *Annu. Rev. Phys. Chem.* **2003**, *54*, 141–172.

(10) Hsu, J.-H.; Fann, W.; Tsao, P.-H.; Chuang, K.-R.; Chen, S.-A. *J. Phys. Chem. A* **1999**, *103*, 2375–2380.

(11) Wood, P.; Samuel, I. D. W.; Schrock, R.; Christensen, R. L. *J. Chem. Phys.* **2001**, *115*, 10955–10963.

(12) Scharsich, C.; Fischer, F. S. U.; Wilma, K.; Hildner, R.; Ludwigs, S.; Köhler, A. Manuscript in preparation, 2015.

(13) Collison, C. J.; Rothberg, L. J.; Treemanekarn, V.; Li, Y. *Macromolecules* **2001**, *34*, 2346–2352.

(14) Scheibe, G. *Angew. Chem.* **1937**, *50*, 212–219.

(15) Cohen, M. D.; Fischer, E. *J. Chem. Soc.* **1962**, 3044–3052.

(16) Rahimi, K.; Botiz, I.; Agumba, J. O.; Motamen, S.; Stingelin, N.; Reiter, G. *RSC Adv.* **2014**, *4*, 11121–11123.

(17) Yamagata, H.; Hestand, N. J.; Spano, F. C.; Köhler, A.; Scharsich, C.; Hoffmann, S. T.; Bäessler, H. *J. Chem. Phys.* **2013**, *139*, 114903.

(18) Khan, A. L. T.; Sreearunothai, P.; Herz, L. M.; Banach, M. J.; Köhler, A. *Phys. Rev. B* **2004**, *69*, 085201.

(19) Lee, C. K.; Hua, C. C.; Chen, S. A. *Macromolecules* **2013**, *46*, 1932–1938.

(20) Peteanu, L. A.; Sherwood, G. A.; Werner, J. H.; Shreve, A. P.; Smith, T. M.; Wildeman, J. *J. Phys. Chem. C* **2011**, *115*, 15607–15616.

(21) De Leener, C.; Hennebicq, E.; Sancho-Garcia, J.-C.; Beljonne, D. *J. Phys. Chem. B* **2009**, *113*, 1311–1322.

(22) Brunner, K.; Tortschanoff, A.; Warmuth, C.; Bäessler, H.; Kauffmann, H. F. *J. Phys. Chem. B* **2000**, *104*, 3781–3790.

(23) Mollay, B.; Lemmer, U.; Kersting, R.; Mahrt, R. F.; Kurz, H.; Kauffmann, H. F.; Bäessler, H. *Phys. Rev. B* **1994**, *50*, 10769–10779.

(24) Herz, L. M.; Silva, C.; Grimsdale, A. C.; Müllen, K.; Phillips, R. T. *Phys. Rev. B* **2004**, *70*, 165207.

(25) Klafter, J.; Shlesinger, M. F. *Proc. Natl. Acad. Sci. U.S.A.* **1986**, *83*, 848–851.

(26) Klafter, J.; Blumen, A. *Chem. Phys. Lett.* **1985**, *119*, 377–382.

(27) Palmer, R. G.; Stein, D. L.; Abrahams, E.; Anderson, P. W. *Phys. Rev. Lett.* **1984**, *53*, 958–961.

(28) Budimir, J.; Skinner, J. L. *J. Chem. Phys.* **1985**, *82*, 5232–5241.

(29) Blumen, A.; Zumofen, G.; Klafter, J. *Phys. Rev. B* **1984**, *30*, 5379–5382.

(30) Klafter, J.; Blumen, A. *J. Chem. Phys.* **1984**, *80*, 875–877.

(31) Mollay, B.; Kauffmann, H. F. *J. Chem. Phys.* **1992**, *97*, 4380–4397.

(32) Williams, G. Molecular aspects of multiple dielectric relaxation processes in solid polymers. *Electric Phenomena in Polymer Science*; Springer: Berlin Heidelberg, 1979; Vol. 33, pp 59–92.

(33) Nicolai, H. T.; Kuik, M.; Wetzelaer, G. A. H.; de Boer, B.; Campbell, C.; Risko, C.; Brédas, J. L.; Blom, P. W. M. *Nat. Mater.* **2012**, *11*, 882–887.

(34) Köhler, A. *Nat. Mater.* **2012**, *11*, 836–837.

(35) Mikhnenko, O. V.; Kuik, M.; Lin, J.; van der Kaap, N.; Nguyen, T.-Q.; Blom, P. W. M. *Adv. Mater.* **2014**, *26*, 1912–1917.

(36) Plumhof, J. D.; Stöferle, T.; Mai, L.; Scherf, U.; Mahrt, R. F. *Nat. Mater.* **2014**, *13*, 247–252.